The Effects of Technological Compatibility for Silicone Rubber/Fluororubber Blends

Dae Hyun Kim,[1] Sung Hyuk Hwang,[2] Bong Shik Kim[1]

[1]*School of Chemical Engineering, Yeungnam University, Gyeongsan 712-749, Korea*
[2]*Sung Jong Company, Deagu University Business Incubating Center, Jillyang, Gyeongbuk 712-714, Korea*

Received 14 January 2010; accepted 20 September 2011
DOI 10.1002/app.35667
Published online 14 January 2012 in Wiley Online Library (wileyonlinelibrary.com).

ABSTRACT: In this study, silicone rubber (SR) and fluororubber (FKM) blends were prepared and their properties were investigated. The crosslinking rate in the blends was increased with increase of SR content due to the silica filler existing into SR. As the content of FKM in the blends increases, the thermal decomposition temperature of the blends tended to increase and the thermal stability of 25/75 SR/FKM blend was higher than that of any other blends ratios. With the increase of FKM content in the blends, the contact angle of SR/FKM blends decreased and the surface energy increased owing to the change of the polarity of the surface. Dynamic mechanical analysis of 25/75 SR/FKM blend showed two transitions peak at −60.5 and −12.7°C, respectively, indicating the immiscibility. Fourier transform infrared attenuated total reflectance studies showed shifts in the peaks due to specific interactions in the blends, and field emission scanning electron microscopy (FE-SEM) studies revealed that the domain sizes of the blends come to be smaller with increasing FKM content. In the blend with 75 wt % of FKM, we observed that it is technologically compatible due to the increase of physical properties and the decrease of the domain size of FE-SEM in 25/75 SR/FKM blend. © 2012 Wiley Periodicals, Inc. J Appl Polym Sci 125: 1625–1635, 2012

Key words: blend; fluororubber; silicone rubber; thermal properties; dynamic properties

INTRODUCTION

The miscibility of polymers until recently has been treated as a special case in the field of polymer blends or alloys. The miscible polymers show definite thermodynamic properties that alter the physicomechanical behavior of the blend. Several miscible blends have been studied in the past decades and the most comprehensive review has been authored by Krouse.[1]

The first commercial success of miscible blend of poly(vinyl chloride) and acrylonitrile butadiene copolymer[2] provoked the development of newer miscible blends consisting of plastic–plastic, plastic–rubber, and rubber–rubber blends. The rubber–rubber blends have been reviewed extensively by Roland[3] and Corish.[4] Miscibility has been reported in few cases. The miscibilities of polyacrylate and polymethacrylate with poly(vinylidene fluoride) have been characterized by several techniques.[5,6]

The poly(vinylidene fluoride) forms blends based on thermodynamic compatibility with certain polymers such as polyacrylates and polymethacrylates.[7] Benedetti et al.[8] have characterized the blends of an acrylic resin with fluoroelastomer based on vinylidene fluoride (VdF) and hexafluoropropene copolymer.

The concept of physically blending two or more existing polymers to obtain a new product has not been developed as fully as the chemical approach to blending, but the physical approach is now attracting widespread interest and is being used commercially. Polymer blends are physical mixtures of structurally different polymers, which interact through secondary forces with no covalent bonding.[9] The manifestation of superior properties depends upon compatibility or miscibility of homopolymers at molecular levels. Compatibility of polymer blends can be examined by sophisticated experimental and theoretical techniques[10–14] to decide their practical activity.

If the mechanical mixing is strong enough and high enough as much as on the whole, then the viscosity after the mixing prevents the phase separation and the rubber blend can obtain the uniform phase.[15] However, Ghosh et al.[16,17] reported that the blends of silicone rubber (SR) and fluororubber (FKM) are thermodynamically immiscible and technologically compatible.

SR excels in high temperature stability, low temperature flexibility, chemical resistance, weatherability, electrical performance, and sealing capability. Compared with many organic elastomers, SR offers superior ease of fabrication resulting in high productivity and cost effectiveness for extended service reliability. Mitchell[18] has reported the improvement in

Correspondence to: B. S. Kim (kimbs@ynu.ac.kr).

tensile strength of ethylene propylene diene monomer (EPDM)/SR blend through interfacial coupling. Kole et al.[19–22] have reported morphology, physical properties, dielectric properties, thermal stability, and effect of compatibilizing agent on blends of EPDM and SR. Bridges et al.[23] have reported that a silicone elastomer can be alloyed with polyester thermosetting resin by a chemical crosslinking process. The resultant material has the impact strength, chemical resistance, and weatherability of SR coupled with mechanical strength, insulating properties, and economic advantage of polyester resins. Falender et al.[24] have prepared the blend of SR with polyethylene using the mechanical shearing process.

FKM is used in many industrial applications such as gaskets, seals, and O-rings in the petrochemical, automotive, and food processing industries. This is due to their unique combinations of mechanical properties coupled with the inherent resistance to fuel, oil, and heat by virtue of the strong nature of its structural chemistry (i.e., C—F bond energy = 485 kJ mol^{-1}).[25] It can be due to higher energy of C—F bonds in FKM compared with bond energy of Si—C (306 kJ mol^{-1}) and C—C (346 kJ mol^{-1}) in other polymers.[26]

However, one disadvantage of the FKM is its lack of low temperature resistance. Thus, to improve its properties, the blending method of FKM has been extensively investigated with a polymer like SR. The preparation of SR/FKM blends, crosslinked by peroxide system, is industrially important and can substitute expensive fluorosilicone rubber.

Therefore, the aim of this study was to investigate the blends of SR/ FKM and to investigate in detail the degree of cure, the contact angle, the surface energy, thermogravimetric analysis (TGA), the change of glass transition temperature (T_g) by dynamic mechanical analyzer (DMA), and phase behavior of the blends and performed the physical properties test to illustrate the technological compatibility about the SR/FKM blends.

EXPERIMENTAL

Materials

Poly(methylvinylsiloxane), namely SR, used in this study was a commercial grade rubber (KE 941-U, hardness = 43 durometer A, plasticizing temperature = 190°C, tear strength = 15 kN m^{-1}, specific gravity = 1.11 g cm^{-3}, tensile strength = 6.5 MPa, and elongation at break = 385%; Shin-Etsu, Chiyoda-ku, Tokyo, Japan). Vinylidene fluoride/hexafluoropropylene/tetrafluoroethylene terpolymer (FKM) used in our study was a commercial grade elastomer (E-18894, specific gravity = 1.75, tensile strength = 16.5 MPa, and elongation at break = 254%; Dyneon, Decatur, Alabama, US). Crosslinking agent commercially known as LS-4 (2,5-bis-(*t*-butylperoxy)-2,5-dimethylhexane) was supplied by Dow Corning, Jincheon-gun, Chungcheongbuk-do, Korea. Coagents were studied by using triallylcyanurate (TAC; 2,4,6-triallyloxy-1,3,5-triazine, Aldrich, Yongin-si, Gyeonggi-do, Korea). Scheme 1 shows the chemical structures of SR, FKM, TAC, and LS-4.

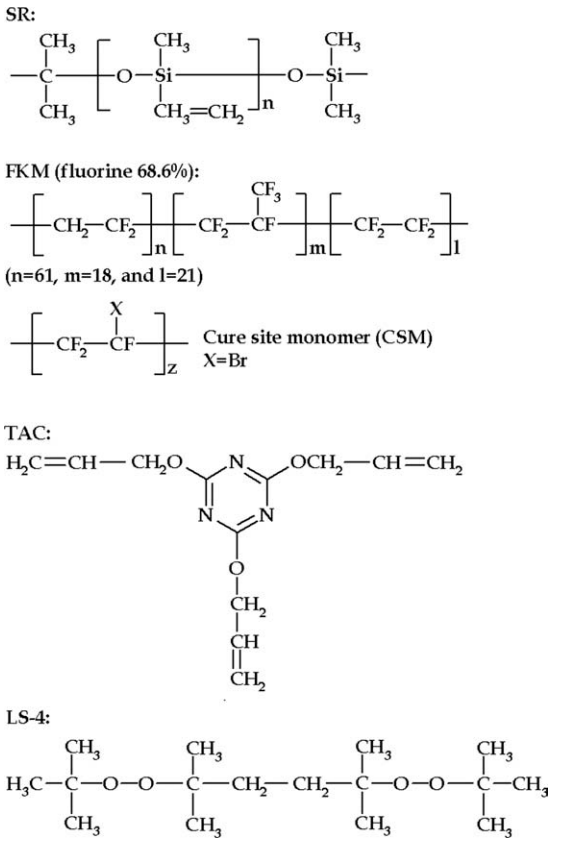

Scheme 1 The chemical structures of SR, FKM, TAC, and LS-4.

As shown in Scheme 1, FKM investigated in this experimental is composed of three components, that is, tetrafluoroethylene, hexafluoropropylene (HFP), and VdF. Tertiary peroxide curable FKM was mainly composed of TFE, HFP, and VdF. In addition to cure site monomer(CSM) is essential for crosslinking. To improve the curability, a CSM has also been included into the chain of FKM. A third functional reactive monomer (CSM) is added in the polymerization to create a crosslinking site on the FKM. In this study, we used tertiary peroxide curable FKM, which has Br CSM. Commonly used SR peroxides include aryl–alkyl derivatives such as dicumyl peroxide and dialkyl derivatives such as 2,5-bis-(*t*-butylperoxy)-2,5-dimethylhexane. The cross-linking of vinyl containing poly(dimethylsiloxane) (PDMS) can be achieved using aryl–alkyl or dialkyl peroxides.[27,28]

Preparation of the samples

SR/FKM blends were prepared at weight ratios of 75/25, 50/50, and 25/75. Rubber blends were

prepared using an internal mixer (HAAKE, Rheocord 9000, Germany) at a rotor speed of 60 rpm at 80°C. FKM was first sheared for 5 min and then SR was added in there and they were mixed for an additional 5 min. Finally, LS-4 and TAC were added in there and they were mixed for another 3 min. After mixing, the blends were formed into sheets in a two-roll open mixing mill at 60°C.

To minimize the influence of processing conditions, the compound was under equally processing time of all specimens and temperature, and so on. The optimum cure time of compounds were measured with using flat die rheometer (FDR). Rubber sheets $\sim$ 2 mm in thickness were prepared using a hot-press with a compression molder at 160°C and a pressure of 15 MPa for 20 min. Compounds used in this study are shown in Table I.

TABLE I
Blend Ratio of SR/FKM

Ingredients	A (phr)	B (phr)	C (phr)	D (phr)	E (phr)
SR[a]	0	25	50	75	100
FKM[b]	100	75	50	25	0
LS-4[c]	2	0.84	0.75	1.07	0.7
TAC 50%[d]	2.5	0.80	0.60	0.54	–

[a] Silicone rubber [KE941-U(SR)].
[b] Fluororubber.
[c] Peroxide (50% active content).
[d] Triallylcyanurate (50% active content).

Instrumentation

An internal mixer (HAAKE, Rheocord 9000) and two open mixing mills were used for mixing and blending. A hot-press was used for compression, heating, and crosslinking. The crosslinked blends were prepared under a pressure of 15 MPa for 20 min. To determine the curing behaviors of the blends, the cure characteristics of the compounds were determined using an Ueshma FDR (Japan) with 3 g samples of the blend compounds at 165°C for 20 min with amplitude angle 1°.

The contact angles of the pure component rubber and blends were determined using a contact angle meter (Kruss, DSA 100, Germany). The sessile drop method[29] was used for the measurements using 2 μL drops of bidistilled water. The contact angle measurements were performed for 10 min after dropping water onto the surfaces of the compounds until a stable value was achieved. Each reported contact angle result is the mean of at least 10 measurements with a standard deviation of ±2°. The surface energies of SR/FKM blends were determined using the Neumann equation.

TGA of samples were performed using a TA Instruments (TA Q 5000) with automatic programmer from a temperature to 800°C and increasing according to at a programmed heating rate of 10°C min^{-1} in a platinum pan under nitrogen flow. A sample with weight of $\sim$ 30 mg was collected for each measurement. The degradation temperature (T_0) and the temperature of maximum weight loss (T_{max}) were evaluated for each sample.

Measurements of dynamic mechanical properties of the blends were performed using a DMA (RSA 3, TA Instruments). The dual cantilever mode of deformation geometer or three-point bending mode was used ranging of −100 to 100°C at a heating rate of 10°C min^{-1} and at a frequency of 10 Hz. The average specimen dimensions were 12 mm in length, 4 mm in width, and 3 mm in thickness. The storage modulus (E') and loss tangent (tan δ) were measured for all samples under identical conditions.

Stress–strain properties were measured according to ASTM D412-98 using a universal testing machine (Instron 5567). All tests were performed at room temperature with a crosshead speed of 500 mm min^{-1}. The averages of five measurements were used to calculate the sample strengths.

Fourier transform infrared attenuated total reflectance (FTIR-ATR) spectra of blends were taken at room temperature using a Jasco FTIR 6200 V spectrophotometer with a 45° KRS5 prism. The specimens were scanned from 4000 to 600 cm^{-1} with a resolution of 4 cm^{-1}. The average of three scans for each sample was taken for the peak identification.

The morphology of blends was investigated by field emission scanning electron microscopy (FE-SEM) using a Jeol instrument model JSM-6701F. Samples were fractured in liquid nitrogen and then coated with gold using a Cressington 108 auto sputter coater. The morphology was determined using an accelerating voltage of 5 kV.

RESULTS AND DISCUSSION

The cure characteristics of blends

Five types of SR/FKM blends were prepared with different weight percentages to examine their cure characteristics. Figure 1 illustrates the method used to record the curing characteristics using a rheometer with ASTM D 2084, and the results are presented in Table II. The torque tended to increase with increasing curing time. Torque of pure SR showed higher torque valves than that of pure FKM. This is owing to the filler (precipitated silica and fumed silica) including in SR. Generally, the filler types of SR are classified into two categories, that is, one is precipitated silica and the other is fumed silica. These have excellent insulating properties, especially under wet conditions.

The torque as a function of time, as shown in Figure 1, required periodic rotation to maintain a

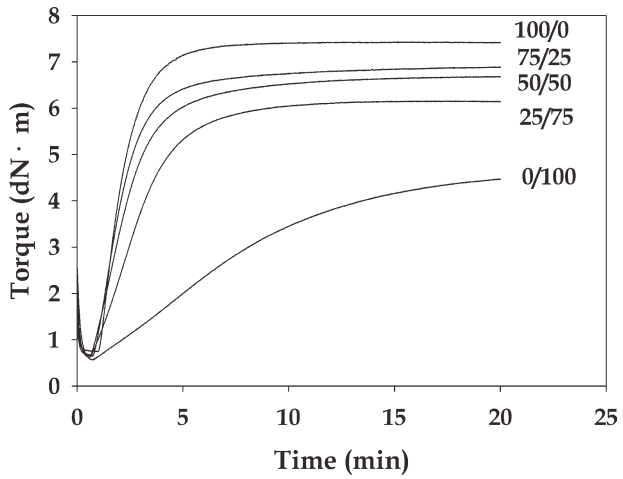

Figure 1 Curing characteristics of SR/FKM blends at 165°C.

constant angle of a disk placed on the center of the rubber sheet. Given a power, namely, a torque is proportionate to the degree of curing and can be obtained using the following equation:[30]

$$\text{Degree of crosslinking } (\%) = \frac{T(t) - T_{\min}}{T_{\max} - T_{\min}} \times 100 \quad (1)$$

where $T_{\max}$ is the value of maximum torque (N·m), $T_{\min}$ is the value of minimum torque, and $T(t)$ is the value of torque at the cure time.

Contact angle measurements and surface energy calculations

When a liquid drop is in contact with an ideally smooth, undeformable, homogeneous solid (Fig. 2), it exhibits an equilibrium contact angle that can be expressed by the Young's eq. (2)[31]:

$$\gamma_{\text{LV}} \cos\theta = \gamma_{\text{SV}} - \gamma_{\text{SL}} - \pi_e \quad (2)$$

where γ_{LV} is the surface tension of the liquid in equilibrium with its own vapor, γ_{SL} is the interfacial tension between liquid and solid, γ_{SV} surface tension of the solid in equilibrium with the saturated liquid

TABLE II
Curing Characteristics of SR/FKM Blends

SR/FKM	$T_{\min}$[a]	$T_{\max}$[b]	t_{10}[c]	t_{50}	t_{90}
0/100	0.56	4.48	1.99	6.50	14.25
25/75	0.62	6.16	1.13	2.73	5.91
50/50	0.67	6.69	1.00	2.19	5.24
75/25	0.65	6.90	1.05	1.97	4.38
100/0	0.74	7.43	1.23	1.97	3.85

[a] Minimum torque value (dN·m).
[b] Maximum torque value (dN·m).
[c] The time to 10% of maximum torque value (min).

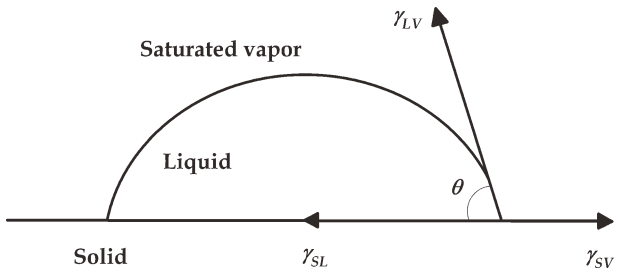

Figure 2 A sessile drop of liquid on a solid showing a three-phase force line.

vapor, and θ the contact angle, and $\pi_e = (\gamma_S - \gamma_{\text{SV}})$, equilibrium pressure. It is generally believed that, if the contact angle is greater than zero, π_e is negligible and $\gamma_S = \gamma_{\text{SV}}$. Therefore, eq. (2) can be rewritten as:

$$\gamma_{\text{LV}} \cos\theta = \gamma_S - \gamma_{\text{SL}} \quad (3)$$

Attempts were made in the literature to modify Berthelot's rule by introducing a modifying factor. Good et al.[32–34] were the first to propose a modifying factor known as Good's interaction parameter, Φ, in the 1950s:

$$\gamma_{\text{SV}} = \gamma_S + \gamma_{\text{LV}} - 2\Phi\sqrt{\gamma_S\gamma_{\text{LV}}} \quad (4)$$

They quantified Φ for various systems using the molar volumes of two phases in contact. In the early 1990s, Li et al.[35,36] proposed an exponential modifying factor $\exp[-\beta(\gamma_{\text{LV}} - \gamma_S)^2]$. Hence an equation of state for interfacial tension was written as:

$$\gamma_{\text{SL}} = \gamma_S + \gamma_{\text{LV}} - 2\sqrt{\gamma_S\gamma_{\text{LV}}}\exp[-\beta(\gamma_{\text{LV}} - \gamma_S)^2] \quad (5)$$

In one-liquid method, the surface energy γ_S was determined using the following Neumann eq. (6).[37,38] In combination with young's equation, one-liquid method enables the solid surface energy to be determined from a single contact angle measurement using only one liquid. Equations (3) and (5) yield:

$$\cos\theta = -1 + 2\sqrt{\frac{\gamma_S}{\gamma_{\text{LV}}}}\exp[-\beta(\gamma_{\text{LV}} - \gamma_S)^2] \quad (6)$$

In Neumann's approach, β is an empirical constant that depends on the system under investigation, but is typically set equal to 0.0001247 $(\text{mJ m}^{-2})^{-2}$.

The values of contact angle measurements for each SR/FKM blend are given in Table III. The contact angle increased only slightly with increasing the content of SR. A photo image results by the sessile drop method using a contact angle meter (Kruss, DSA 100, Germany). The contact angle of the pure FKM and SR were 100.2° and 122.0°, respectively, and Table III indicated that the contact angle values

TABLE III
Measurement Contact Angle Values for SR/ FKM Blends

SR/FKM	Contact angle (°)
75/25	124.4
50/50	121.5
25/75	115.8

were decreased with increasing the content of FKM owing to the polar of the surface of the pure FKM.

The surface energy calculations for all SR/FKM blends are summarized in Table IV. The surface energies of the SR/FKM blends were calculated using the Neumann eq. (6).[36] The surface energy decreased with increasing contact angle and the surface energy of the pure FKM and SR were 22.92 and 10.57 mJ m^{-2}, respectively. The surface energy was decreased with increasing the content of SR in the blends and the surface energies of 25/75, 50/50, and 75/25 SR/FKM blends were 13.82, 10.82, and 9.39 mJ m^{-2}, respectively. The surface energy increased with decreasing the contact angle and SR content in the blends. Table IV is surmised that the surface is changed into the polarity.

Thermal properties

The thermal properties of blends were evaluated using thermogravimetric analyzer (TGA). Figure 3 shows the TGA results for all SR/FKM blends, and Figure 4 shows derivative thermogravimetric (DTG) results. TGA analyses were carried out in the temperature ranges from 80 to 800°C.

The TGA curve of the 50/50 SR/FKM blend in Figure 3 shows that SR undergoes two stages thermal degradation, between 330 and 465°C and again between 465 and 583°C. The weight loss during the first stage is attributed to the loss of volatile products formed during the degradation process. The weight loss in the second stage is attributed to the formation of carbonaceous residue and silica filler. The 25/75 SR/ FKM blend also exhibited two-step thermal degradation, which occurred between 340 and 448°C and between 448 and 541°C. However, with increase of FKM content, the onset degradation was increased from 330°C (50 wt % FKM) to 340°C (75 wt % FKM), while the onset degradation occurred at 320°C in the FKM. The significant increase in degradation temperature is probably due

TABLE IV
Surface Energies (γ_S) of SR/FKM Blends Using One-Liquid Method

SR/FKM	γ_S (mJ m^{-2})
75/25	9.39
50/50	10.82
25/75	13.82

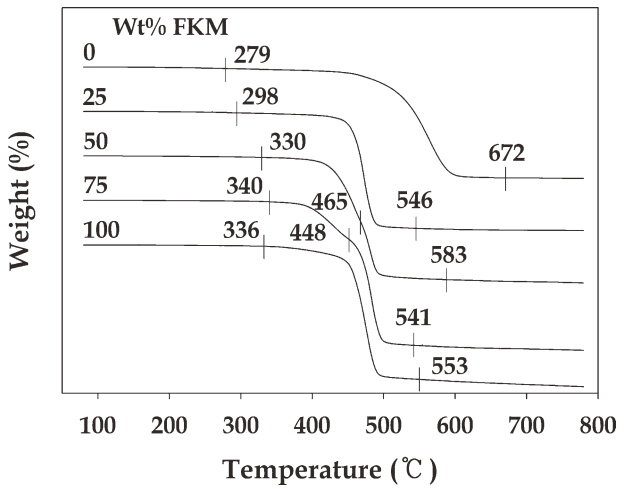

Figure 3 TGA curves of SR/FKM blends.

to the effect of silica filler existing into the SR. Thus, the SR/FKM blends had higher degradation temperatures than did the FKM. In the case of 25 wt % FKM, only single step degradation was found in the temperature range of 298–546°C. The marked difference in the thermal properties of these blends indicate that the degradation temperature of SR is higher than that of FKM, where its defluorination occurs.

From Figure 3, the initial degradation temperatures corresponding to 1% decomposition for the pure FKM and SR were 336 and 279°C, respectively. FKM has the higher degradation temperature than that of SR owing to the highest bond dissociation energy of FKM. Also, with increase of FKM content, the thermal degradation temperature showed the tendency to increase and the 25/75 SR/FKM blend showed the higher thermal stability than that of the other blend samples. This is due to the higher bond energy of C—F existing into the FKM.

The two stages thermal degradation observed in the SR/FKM blends were also well reflected in the DTG

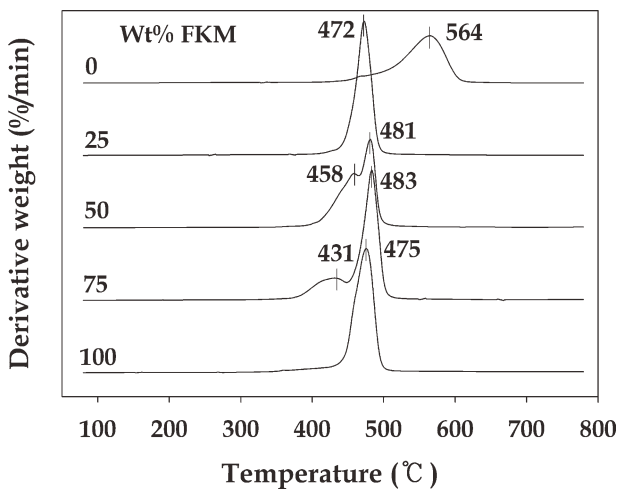

Figure 4 DTG curves of SR/FKM blends.

TABLE V
Thermal Properties of Blends

SR/FKM	TGA temperature (°C), 1 wt % loss	DTG degradation, wt % loss
100/0	279 (565)[a]	49.6[b]
75/25	298 (474)[a]	44.3[b]
50/50	330 (473)[a]	33.6[b] (63.8)[c]
25/75	340 (476)[a]	17.7[b] (66.6)[c]
0/100	336 (473)[a]	56.1[b]

[a] Temperature for 50% weight loss.
[b] Wt % loss for the first thermal degradation.
[c] Wt % loss for the second thermal degradation.

curves shown in Figure 4. The weight loss to area under the first peak was less than that under the second peak, which indicates that the weight loss in the second peak is higher for SR. The incorporation of FKM into SR matrix showed two-step degradation processes. However, the incorporation of FKM showed a new derivative peak significantly at a higher temperature apart from the derivative peak corresponding to the SR. It is thought that the introduction of FKM enhanced the thermal stability of SR matrix.

In the DTG curves of Figure 4, blends of the SR with 50 and 75 wt % FKM also showed two-step thermal degradation processes, which occurred in the temperature 458 and 481°C for 50 wt % FKM and 431 and 483°C for 75 wt % FKM in the first and second steps, respectively. Figure 4 showed the temperature transformation at the highest inflection point of the first thermal degradation processes in the derivative curves. In the case of low content of 25 wt % FKM, the temperature curves at the highest inflection point of the DTG curves indicated single peak. In Figure 4, it is thought that the DTG curve of the 75/25 SR/FKM blend indicated the single peak because the temperature of the DTG curve of pure SR is higher than that of pure FKM and the 75/25 SR/FKM blend contains the lower content of FKM.

The lower initial degradation of SR compared with the other samples is thought by decomposition of cyclic silicone oligomers and also lower bond energy (Si—C = 306 kJ mol^{-1}).[26] It has been reported that SR consists of cyclic dimethylsiloxane (DMS), and a small amount of linear DMS (≈1 wt %) form the thermal degradation of PDMS.[26] The molecular units of most formed cyclic DMS (≈90 wt %) are 3–6 (D_3–D_6).[39–42] Low unit silicone oligomers dominate low boiling temperature with those of D_4–D_6 ranging from 173 to 245°C. Therefore, these oligomers are volatilized due to thermal effects. The temperature required to result in 1 and 50% weight losses and the percentage weight loss for the second thermal degradation are summarized in Table V.

Degradation began earlier in the SR and the FKM than in the SR/FKM blends. Similar behavior has been observed in many miscible blends in which one of the components is more prone to degradation than are the others.[43] The temperature required for 50% weight loss was more or less the same for all the blends and individual components. As shown in Table V, the 25/75 SR/FKM blend is more stable due to the higher temperature of degradation and the lower wt % loss for thermal degradation. It is thought that the 25/75 SR/FKM blend showed better technological compatibility.

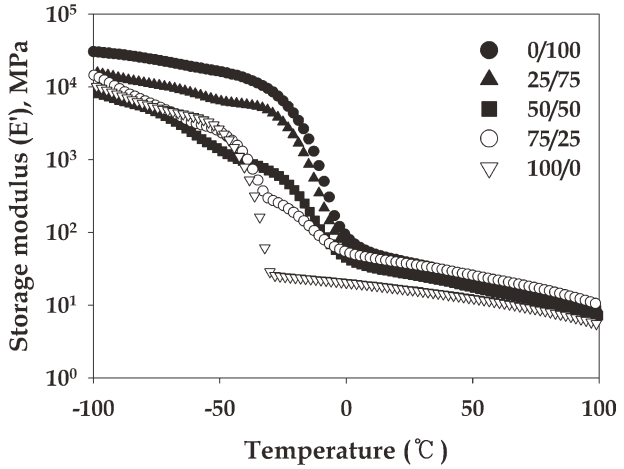

Figure 5 Storage modulus (E') of SR/FKM blends.

DMA analysis

Dynamic mechanical analysis is a versatile and sensitive tool enabling a complete exploration of relaxation mechanisms in viscoelastic materials, especially polymer blends. The most common use of DMA is the determination of the glass transition temperature (T_g), at which the molecular chains of a polymer obtain sufficient energy, usually from thermal sources, to overcome the energy barriers for segmental motion.

The storage modulus (E') and loss factor (tan δ) of all the samples are illustrated in Figures 5–7. The magnitude and nature of the change in the dynamic modulus of elasticity are determined by

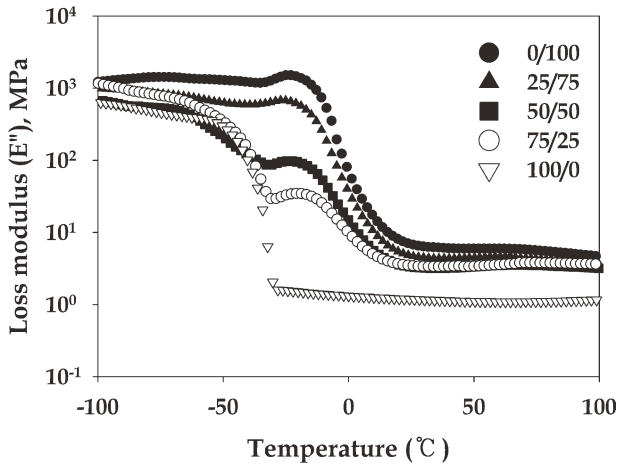

Figure 6 Loss modulus (E'') of SR/FKM blends.

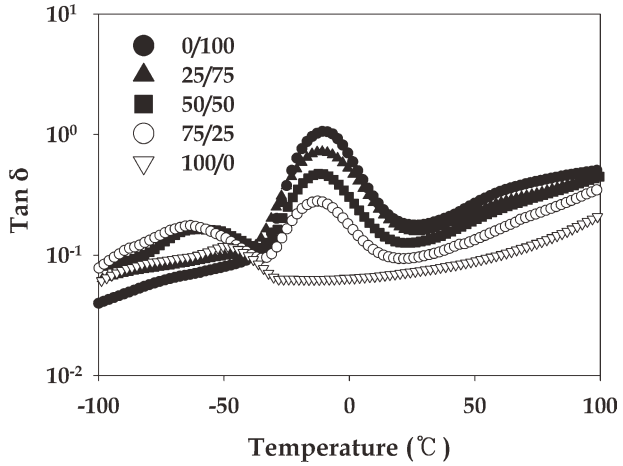

Figure 7 Tangent (tan δ) of SR/FKM blends.

intermolecular interactions. The latter has greater influence in the different physical states of the polymer.[44] In the glassy state, when the intermolecular interactions are sufficiently great, the dynamic storage modulus is $\sim 10^9$ Pa. However, in the rubbery state, when the energy of intermolecular interactions is appreciably lower, the dynamic modulus of the same polymer is $\sim 10^6$ Pa. Any change in the energy of intermolecular interactions, which affect molecular motion in polymers, also will have an appreciable influence on the magnitude and nature of the modulus.

Figure 5 illustrates that the storage modulus of the SR slightly was enhanced with the addition of 25 wt % FKM, and that E' increased with increasing FKM content. This improvement in E' is due to the high modulus of FKM phase. In polymer blends, DMA shows a single transition between the individual values of T_g, if the two components are fully miscible and only one phase exists. On the other hand, if the two polymers are immiscible and two distinct phases exist, then the blends will show two distinct peaks. If the polymer blends are partially compatible, their T_g values will shift toward each other.[43]

Figure 7 shows the tan δ temperature curves of the SR/FKM blends. The pure FKM has T_gs of −12.2°C. The 25/75 SR/FKM blend had two glass transition temperatures of −60.5 and −12.7°C, which indicates the immiscibility of the two components with these blend ratios. The other two blends showed two peaks, with main peak due to the FKM and the shoulder due to SR. Both peaks were shifted toward each other with respect to the individual T_g. This indicates partial miscibility for the 50/50 SR/FKM and 75/25 SR/FKM blends. The peak temperature values are listed in Table VI.

TABLE VI
Thermomechanical Properties of the SR/FKM Blends

SR/FKM	Temperature for tan δ_{max} (°C, from DMA)
100/0	−124.4[a]
75/25	−63.3[b] (−14.7)[c]
50/50	−63.3[b] (−13.6)[c]
25/75	−60.5[b] (−12.7)[c]
0/100	−12.2[c]

[a] Value assessed by DSC.
[b] SR transition.
[c] FKM transition.

Physical properties

Effects of the blend ratio on the physical properties of the SR/FKM blends are shown in Figures 8 and 9(a,b) and their physical properties are summarized in Table VII.

The modulus increased and the tensile strengths increased in the 25/75 SR/FKM and 50/50 SR/FKM blends. In the 25/75 SR/FKM blend, tensile strength and elongation at break were larger than those of 50/50 SR/FKM. The better tensile strength of 25/75 SR/FKM blend may be attributed to the increase of the technological compatibility. On the basis of processing, curing characteristics, and final properties, it appears that SR, which is of much lower viscosity than that of the FKM, forms the continuous phase in the blend, particularly at FKM concentrations of 50% and above. It is also evident that synergism in properties becomes prominent at higher FKM concentrations. Results of physical properties measurements reveal that the blends of SR and FKM are technologically compatible. Technological compatibility means efficient stress transfer from one phase to another phase, resulting in improved physical properties as observed in the present case. If the blends were technologically incompatible, the physical properties would have fallen.

FTIR-ATR analysis

FTIR has used as a powerful tool for studying polymer blend miscibility. If a blend is miscible or

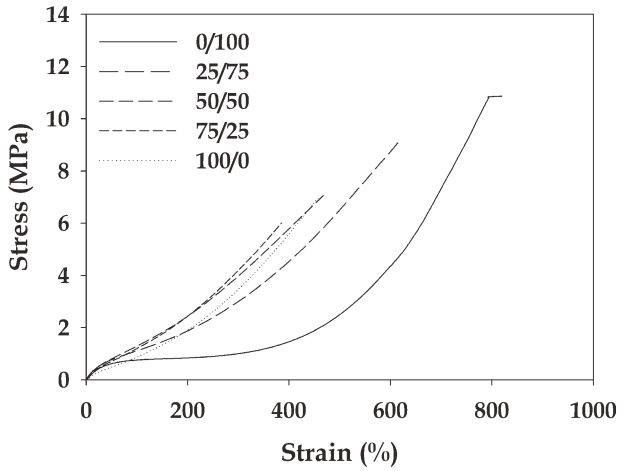

Figure 8 Stress-strain plots of the SR/FKM blends at room temperature.

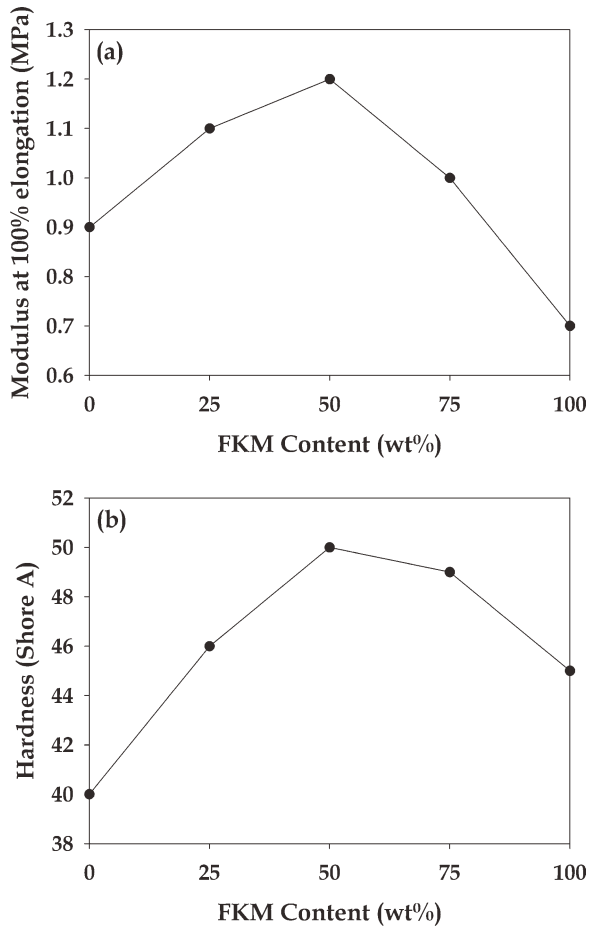

Figure 9 Physical properties of SR/FKM blends: (a) variation of modulus at 100% elongation with blend composition and (b) variation of hardness with blend composition.

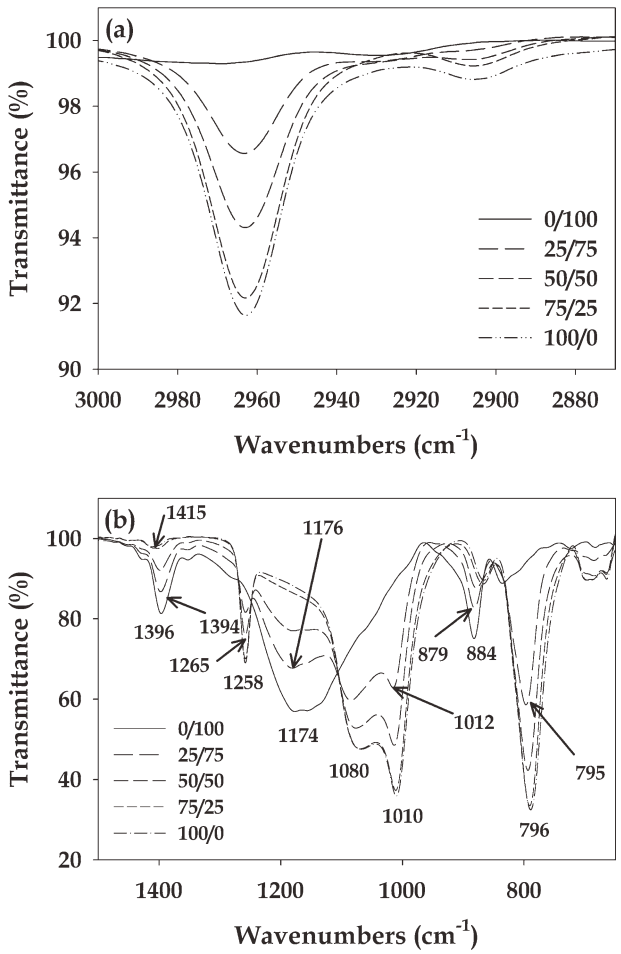

Figure 10 FTIR-AIR spectra of SR/FKM blends: (a) 3000–2870 cm^{-1} of the wave numbers scale; (b) 1500–650 cm^{-1} of the wave numbers scale.

partially miscible, a specific interaction in the blend disrupts the bonding between the atoms and a difference can be seen in the absorption spectrum. On the other hand, if a blend is immiscible, the absorption spectrum of the blend will be the sum of the individual components.[43,45]

FTIR spectra of the pure polymers and the blends are given in Figure 10(a,b). The pure FKM showed three absorption peaks: the strongest band at 1174 cm^{-1} by $\nu(CF_2)$ stretching vibrations, the band at 1396 cm^{-1} by ν(CF), and the other band around 884 cm^{-1} reveals $\nu(CF_3)$ for the FKM. These are the main characteristic bands of pure FKM rubber.[46–51] The absorption bands at $\sim$ 1010 cm^{-1} are the characteristic absorption bands for —Si—O—Si— group of PDMS polymers. The —Si—O—Si— absorption appeared at 1080 and 1010 cm^{-1}. The distinctive adsorption bands at 1415 cm^{-1} (asymmetric deformation vibrations of the Si—CH_3), 1258 cm^{-1} (symmetric deformation vibrations of the Si—CH_3), 879 cm^{-1} (stretching vibrations of the Si—C), 2962 cm^{-1} (asymmetric stretching vibrations of the C—H), and 2900 cm^{-1} (symmetric stretching vibrations of the C—H) can also be found.

For the SR/FKM blends, the major peaks appear at, for example, 1265, 1176, 1080, 1012, 879, and 795 cm^{-1}. The peaks in the blends slightly shift to a lower wavenumbers because of the specific interaction between the individual components. The peak at 1396 cm^{-1} for FKM shifted to 1394 cm^{-1} in the blends. The peak at 1415 for SR shifted to a lower wavenumbers in the blends. Similarly, the peak at

TABLE VII
Effect of Blend Ratio on the Physical Properties

Physical properties	Silicone rubber/fluororubber (parts by weight)				
	0/100	25/75	50/50	75/25	100/0
Modulus at 100% elongation (MPa)	0.7	1.0	1.2	1.1	0.9
Modulus at 200% elongation (MPa)	0.8	1.8	2.3	2.3	1.9
Tensile strength (MPa)	9.1	7.8	6.7	4.0	6.6
Elongation at break (%)	766	580	468	296	441
Hardness (Shore A)	45	49	50	46	40

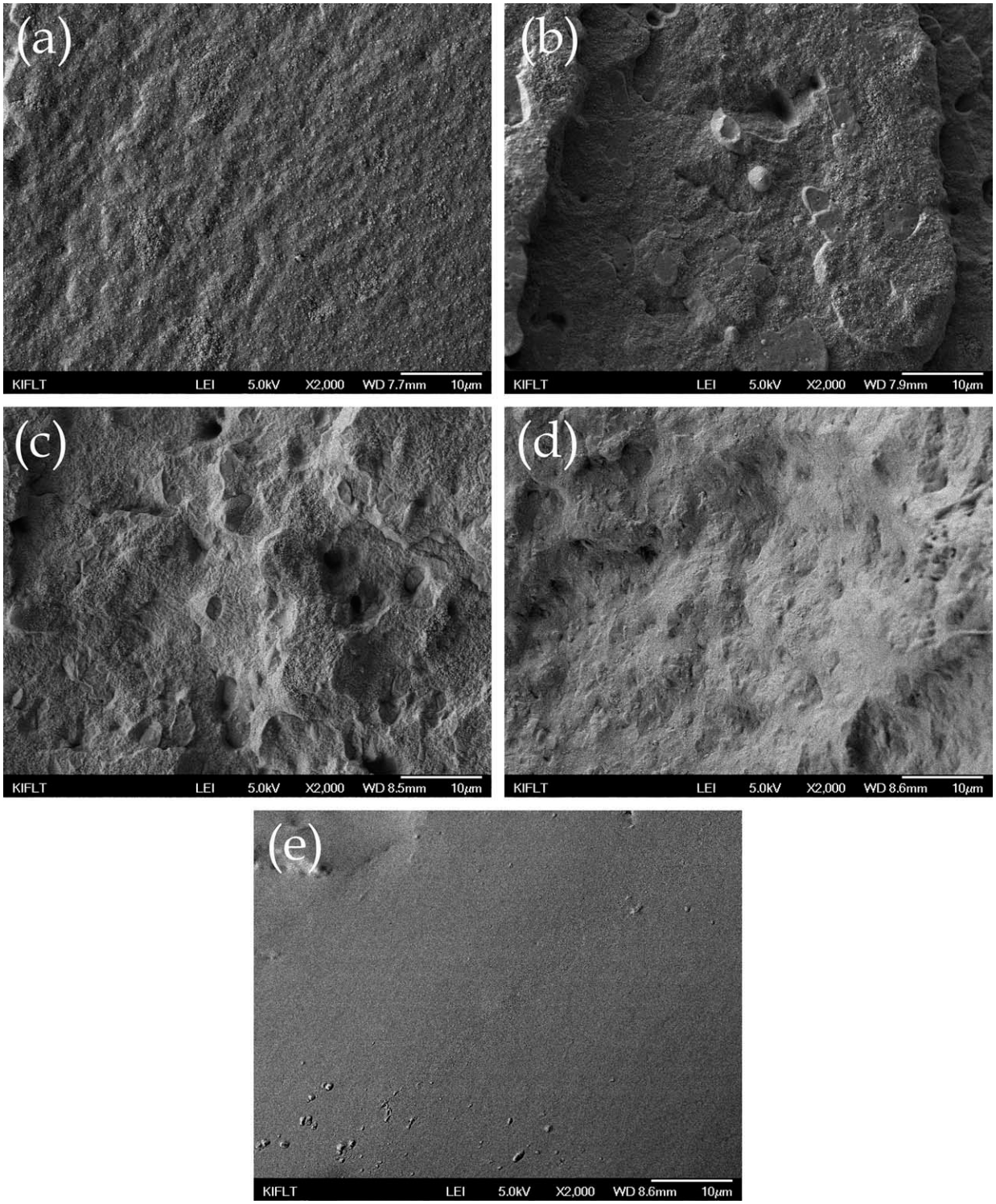

Figure 11 FE-SEM micrographs for SR/FKM blend: (a) 100/0; (b) 75/25; (c) 50/50; (d) 25/75; and (e) 0/100.

879 cm^{-1} for SR/FKM shifted to a lower wavenumbers in the blends.

Morphology observation

Figure 11(a–e) shows FE-SEM micrographs of the SR/FKM blends. The pure FKM showed a comparatively smooth surface with dispersed particles on the surface Figure 11(e). FE-SEM images shows dispersion of FKM domain in the SR matrix. With increase in FKM content, the domain size of second phase decreases as seen in Figure 11(b–d). As shown in Figure 11, with increase of the SR content, the domain size was increase and the 25/75 SR/FKM

blend exhibited smaller domain size than that of the 75/25 SR/FKM blend.

Therefore, we found that blend with 75 wt % FKM is technologically compatible due to interaction between SR and FKM from FE-SEM images. Ghosh and De[52] have reported that the 50/50 blend of SR and FKM is technologically compatible.

CONCLUSIONS

In this study, SR and FKM blends were prepared by various weight percentages. The curing characteristics, contact angle measurements, surface energy calculations, thermal properties, FTIR-ATR analysis, and morphology properties of SR/FKM blends were investigated. The curing rate was quickened by the silica filler existing within SR with increasing SR content. The torque of the SR/FKM blends decreased with increasing FKM content and with transforming phase from the disperse phases to the continuance phases. This means that the change of torque is owing to decrease intermolecular interaction due to weakness than the effect of filler existing within SR with increasing FKM content. The values of contact angle of the blends were increased only a small difference with increasing the content of SR and surface energy calculated by the Neumann equation was increased with decreasing the contact angle and SR content in the blends. This means that the surface is transformed into polarity. Thermogravimetry of the blends showed that degradation occurred between the decomposition of SR/FKM blends. The TGA thermograms indicate the improvement in the thermal stability of the blends owing to incorporation of FKM and thermal stability of SR/FKM blend ratio 25/75 was higher than that of the other blends. Dynamic mechanical analysis showed interactions between the blends. In the 25/75 SR/FKM blend, tensile strength and elongation at break were larger than those of 50/50 SR/FKM. The better tensile strength of 25/75 SR/FKM blends may be attributed to the increase of the technological compatibility. FTIR analysis revealed the existence of specific intermolecular interactions. The morphology of the blends showed the decrease in domain size with increase of FKM content, which implies variation in compatibility.

Consequently, the SR/FKM blends were increased with the compatibility of the blend by co-crosslinker. As the content of FKM in the blends increases, the viscosity of blend increases. The 25/75 SR/FKM blend becomes a homogeneous phase due to these increase of viscosity high enough to prevent the phase separation of blend and it seems that the compatibility of the blend progressively increased.

References

1. Krouse, S. In Polymer Blends; Paul, D. R., Newman, S., Eds.; American Academic Press: New York, 1978; p 2.
2. Zakrzewski, G. A. Polymer 1973, 14, 348.
3. Roland, C. M. In HandBook of Elastomers; Bhowmick, A. K., Stephens, H. L.; Eds.; Marcel Dekker Inc: New York, 2000; p 197.
4. Corish, P. J. In Science and Technology of Rubbers; Eirich, F. R., Mark, J. E., Erman, B., Eds.; Academic Press: New York, 1994; p 545.
5. Paul, D. R.; Barlow, J. W.; Bernstein, R. E.; Wahrmund, D. C. Polym Eng Sci 1978, 18, 1225.
6. Bernstein, R. E.; Cruz, C. A.; Paul, D. R.; Barlow, W. W. J Polym Prepr Am Chem Soc Div Pol Chem 1977, 37, 574.
7. Drobny, J. G. Macromol Symp 2001, 170, 149.
8. Benedetti, E.; Alessio, A. D.; Ziri, M. F.; Bramati, E.; Tirelli, N; Vergamini, P; Moggi, G. Polym Inter 2000, 49, 888.
9. Shen, M.; Kawai, H. Am Chem Eng J 1978, 24, 1.
10. Krause, S. Polymer Blends; In Paul, D. R., Newman S., Eds.; Academic Press: New York, 1978; p 15.
11. Singh, Y. P.; Singh, R. P. Eur Polym J 1983, 19, 529.
12. Singh, Y. P.; Das, S.; Maiti, S.; Singh, R. P. J Pure Appl Ultrasonic 1981, 3, 1.
13. Hourston, D. J.; Hughes, I. D. Polymer 1978, 19, 1181.
14. Sidkey, M. A.; Abd El-Fattah, A. M.; Yehia, A. A.; Abd El-All, N. S. J Appl Polym Sci 1991, 43, 1441.
15. Corish, P. J.; Powell, B. D. W. Rubber Chem Technol 1974, 47, 481.
16. Ghosh, A.; Antony, P.; Bhattacharya, A. K.; Bhowmick, A. K.; De, S. K. J Appl Polym Sci 2001, 82, 2326.
17. Ghosh, A.; Naskar, A. K.; Khastgir, D.; De, S. K. Polymer 2001, 42, 9847.
18. Mitchell, J. M. Rubber Plast News 1985, 3, 18.
19. Kole, S.; Bhattacharya, A. K; Bhowmick, A. K.; Plast Rubber Comp Proc Appl 1993, 19, 117.
20. Kole, S.; Bhattacharya, A. K.; Tripathy, D. K.; Bhowmick, A. K. J Appl Polym Sci 1993, 48, 529.
21. Kole, S.; Chaki, T. K.; Bhowmick, A. K.; Tripathy, D. K. Polym Deg Stab 1993, 41, 109.
22. Kole, S.; Khastgir, D.; Tripathy, D. K.; Bhowmick, A. K. Die Angew Makromol Chem 1995, 21, 225.
23. Bridges, R. D.; Swincer, A. G.; Strudwick, K. R. Silicone Elastomer Polyester Alloy-New Polyester Formed from Tow Thermoset System, The Society of the Plastics Industry Inc: Washington, DC, 1987; p 2.
24. Falender, J. R.; Lindsey, S. E.; Saam, J. C. Polym Eng Sci 1976, 16, 54.
25. Ameduri, B.; Boutevin, B.; Kostov, G. Prog Polym Sci 2001, 26, 105.
26. Clarson, S. J.; Semlyen, J. A. Siloxane Polymers; PTR-Prentice Hall: New Jersey, 1993.
27. Noll, W. Chemistry and Technology of Silicones; Academic Press: New York, 1978.
28. Marsden, J. U.S. Pat. 2, 445, 794 (1948).
29. Wu, S. Polymer Interface and Adhesion; Marcel Dekker Inc: New York, 1982, p 105.
30. Cho, D. W.; Yoon, C. H. J Kor Inst Rubber Ind, 1992, 27, 275.
31. Good, R. J. In: Mittal K. L., ed. Contact Angle, Wettability and Adhesion; Utrecht: VSP, 1993, p 3.
32. Girifalco, L. A.; Good, R. J. J Phys Chem 1957 61, 904.
33. Good, R. J.; Girifalco, L. A.; Kraus, G. J Phys Chem 1957, 62, 1418.
34. Good, R. J.; Girifalco, L. A. J Phys Chem 1960, 64, 561.
35. Li, D.; Neumann, A. W. J Colloid Interface Sci 1990, 137, 304.
36. Li, D. Ph.D. Thesis, University of Toronto, 1990.
37. Li, D.; Neumann, A. W. J Colloid Interface Sci 1990, 137, 324.
38. Neumann, A. W.; Good, R. J.; Hope, C. J.; Sejpal, M. J Colloid Interface Sci 1974, 49, 291.

39. Kumagai, S.; Yoshimura, N. IEEE Trans Dielectr Electr Insulat 2001, 8, 203.
40. Patnode, W.; Wilcock, T. C. Methylpolysiloxanes. J Am Chem Soc 1946, 68, 358.
41. Thomas, T. H.; Kendrick, T. C. J Polym Sci Part A 1969, 7, 537.
42. Kleinert, J. C.; Weschler, C. J. Anal Chem 1980, 52, 1245.
43. Paul, D. R.; Newman, S. Polymer Blends; Academic: New York, 1978; Vol.1.
44. Iperepechko, I. Acoustic Methods of Investigating Polymers; Mir: Moscow, 1975.
45. Utracki, L. A. Polymer Alloys and Blends; Hanser: Munich, 1989.
46. Cuccuru, A.; Sodi, F. Thermochim Acta 1975, 12, 281.
47. Sugama, T. Mater Lett 2001, 50, 66.
48. Harwood, H. J. J Test Eval 1983, 11, 289.
49. Mitra, S.; Ghanbari-Siahkali, A.; Kingshott, P.; Almdal, K.; Rehmeier, H. K.; Christensen, A. G. Polym Degrad Stab 2004, 83, 195.
50. Theodore, A. N.; Carter, R. O. III. J Appl Polym Sci 1993, 49, 1071.
51. Church, J. F.; Evans, D. J. J Appl Polym Sci 1995, 57, 1585.
52. Ghosh, A.; De, S. K. Rubber Chem Technol 2004, 77, 856.